Alfvén eigenmodes driven by energetic ions in JT-60U

K. Shinohara 1), Y. Kusama 1), G. J. Kramer 2), M. Takechi 1), A. Morioka 1), M. Ishikawa 1), N. Oyama 1), K. Tobita 1), T. Ozeki 1), S. Takeji 1), S. Moriyama 1), T. Fujita 1), T. Oikawa 1), T. Suzuki 1), T. Nishitani 1), T. Kondoh 1), S. Lee 1), M. Kuriyama 1), N. N. Gorelenkov 2), R. Nazikian 2), C. Z. Cheng 2), G. Y. Fu 2), A. Fukuyama 3) and the JT-60 Team 1)

1)Naka Fusion Research Establishment, Japan Atomic Energy Research Institute
2)Princeton Plasma Physics Laboratory
3)Kyoto University

e-mail contact of main author: shinohak@fusion.naka.jaeri.go.jp

Abstract. Instabilities with frequency chirping in the frequency range of Alfvén eigenmodes have been found in the domain of $0.1\% < \langle\beta_h\rangle < 1\%$ and $v_{b//}/v_A \sim 1$ with high energy neutral beam injection in JT-60U. One instability appears with frequency inside the Alfvén continuum spectrum and its frequency increases slowly to the Toroidicity induced Alfvén eigenmodes (TAE) gap in an equilibrium change time scale of $\sim$ 200 ms. Another instability appears with frequency inside the TAE gap and its frequency changes very fast by 10 – 20 kHz in 1 – 5 ms. During the occurrence of Fast FS modes, abrupt large-amplitude events often appears with an enhanced drop of neutron emission rate and increase in fast neutral particle fluxes. The loss of energetic ions increases with the peak fluctuation amplitude of $\tilde{B}_\theta/B_\theta$. Energy dependence of loss ions is observed and suggests the resonant interaction between energetic ions and a mode.

1 Introduction

Instabilities in the Alfvén Eigenmodes (AEs) range of frequencies can cause enhanced loss of α particles in burning plasmas with a high α particle pressure gradient and can prevent the plasma from sustaining the fusion burn [1]. The enhanced α loss can also damage the first wall. The understanding of the enhanced fast particle loss caused by AEs is one of the most important issues for an operation of fusion reactors. So far, only a limited parameter domain in the $v_{b//}/v_A$ (the ratio of parallel beam ion velocity to the Alfvén velocity) and $\langle\beta_h\rangle$ (volume averaged hot ion β) space has been studied as shown in FIG. 1. TAE experiments by α particles in TFTR were mostly performed with low $\langle\beta_h\rangle$. At high $\langle\beta_h\rangle$, chirping modes were observed in DIII-D [2].

In JT60U, the regime of $0.1\% < \langle\beta_h\rangle < 1\%$ and $v_{b//}/v_A \sim 1$ has been covered recently with the Negative-ion-based Neutral Beam (N-NB) of $E_{beam} \sim 360$ keV in order to assess the AE activity and the effect of AEs on the loss of energetic ions in the ITER relevant domain. In the N-NBI experiments, we can also study in the birth domain of the ITER α particles.

AE instabilities with frequency sweeping has been observed in the domain [3]. In this paper, we report the characteristics of these instabilities in detail. We also report a loss of energetic ions caused by these instabilities. Energy dependence of fast neutral particle fluxes is observed and suggests the resonant interaction between energetic ions and a mode.

2 Characteristics of instability with frequency sweeping

In FIG. 2, typical time traces of plasma parameters and a frequency spectrum of magnetic fluctuations of an N-NBI experiment are shown. One instability appears with a frequency of about 30 kHz at about 3.8 s and its frequency chirps up to 65 kHz at about 4 s. We label this type of instability as a "slow frequency sweeping (Slow FS)" mode. After 4.1 s, instabilities with fast FS start to develop with a frequency around 60 kHz and chirping by 10 – 20 kHz in 1 – 5 ms. These Fast FS modes continue to be excited intermittently for several hundred milliseconds. These instabilities with frequency sweeping is not observed only with P-NB injection in the similar discharge condition. As can be seen in FIG. 1, both the Slow and the Fast FS modes were observed in the birth domain of ITER alpha particles.

2.1 Instability with slow frequency sweeping

Slow FS modes, introduced in FIG. 2, appear at 0.1 to 0.2 s after the N-NB injection and their amplitude increases as the frequency increases. The amplitude of the Slow FS modes decreases again when the frequency reaches its maximum. As also shown in FIG. 3, Slow FS modes consist of a sequence of short lived modes which have a typical life span of about 10 ms and the same toroidal mode number (n = 1). The amplitude of each short lived mode also

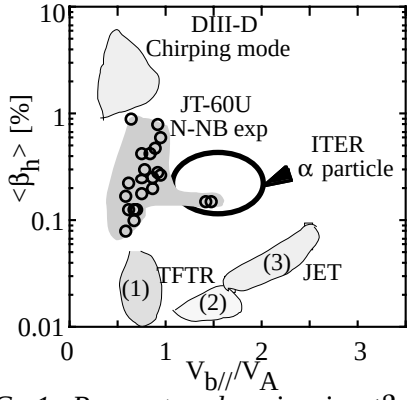

FIG. 1. Parameter domains in $<\beta_h>$ and $V_{b//}$ / V_A space of Alfvén Eigenmode experiments performed in large tokamaks. Open circles show JT-60U experiments that observed AE instabilities with frequency sweeping by employing N-NB. Also shown are an expected α particle parameter domain in ITER, a DIII-D fast ion parameter domain where "Chirping modes" with frequency sweeping in 1 - 10 ms were observed, and α particle parameter domains (1),(2) in TFTR DT experiments, and (3) in JET DT experiments. TAE was observed in (1), but not observed in (2) and (3).

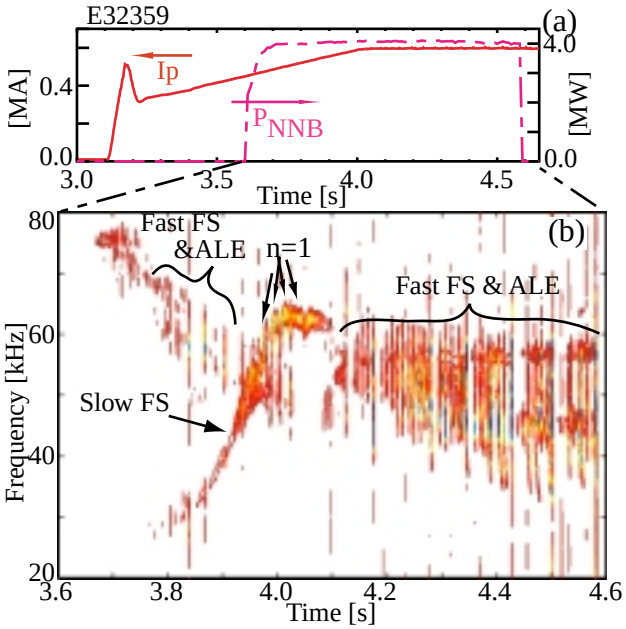

FIG. 2. (a): Time traces of Ip, power of N-NB. (b): Time trace of frequency spectrum of magnetic fluctuations measured by Mirnov coils at the first wall on a midplane. The discharge (E32359) gas is deuterium and the N-NB ion species is deuterium. B_t=1.2T and q_s~5. The N-NB is injected in the co-direction.

increases as its frequency increases. In the discharge E32359, the electron density increased by 50 % from 3.8 to 4.0 s, so the Alfvén gap frequency decreases by about 20 %. The decrease of the mode frequency at around 60 kHz in this time interval is consistent with decrease in the gap frequency. The Slow FS mode does not follow the the Alfvén velocity scaling but it chirps up to the TAE frequency [4].

In FIG. 3, the traces of frequency spectra of magnetic fluctuations are shown in two sequential discharges in which only the N-NBI start time was varied. In the discharge E36379 (case b), the N-NBI was delayed by 130 ms compared to the discharge E36378 (case a). The start frequency of Slow FS modes is $\sim$ 30 kHz in the case (a) and $\sim$ 50 kHz in the case (b). The frequencies of Slow FS modes for both cases at 3.75 s are similar, $\sim$ 50 kHz, even though the N-NB injection was delayed by 130 ms in the case (b) and $\langle\beta_h\rangle$ of the case (a) is larger than that of the case (b) at 3.75s. The frequency of Slow FS modes seems to correlate with the bulk equilibrium parameter variation. On the other hand, the amplitude of Slow FS modes in the case (b) is weaker than that in the case (a) at around 3.75 s, which is considered to be mainly due to a lower $\langle\beta_h\rangle$.

2.2 Instability with fast frequency sweeping

Fast frequency sweeping (Fast FS) modes shown in FIG. 2 exist during a short time span of 1 to 5 ms. An expanded view of some Fast FS modes for a different discharge (E36379) is shown in FIG. 4(a). Most Fast FS modes consist of bifurcating branches with the same start frequency, but some branches chirp up in frequency whereas the others chirp down on a time scale of 1 to 5 ms. In FIG. 4(b), a filtered magnetic probe signal versus time, filtered with a frequency of 30 – 60 kHz bandwidth, is shown for a Fast FS mode. We can see a waveform of beat waves due to the multiple branches of Fast FS modes. The shorter time scale of the beat means the increase in the difference in mode frequency. The time scale of frequency sweeping of Fast FS mode is shorter than 5 ms. It is difficult to explain the frequency sweeping by the equilibrium parameter variation. A possible explanation of Fast FS mode is a change of particle distribution [5–7].

2.3 Abrupt large-amplitude event

Another new type of wave activity is the abrupt large-amplitude events (ALEs). Figure 5(a) shows the time trace of magnetic fluctuation amplitude in the frequency range of 30 –70

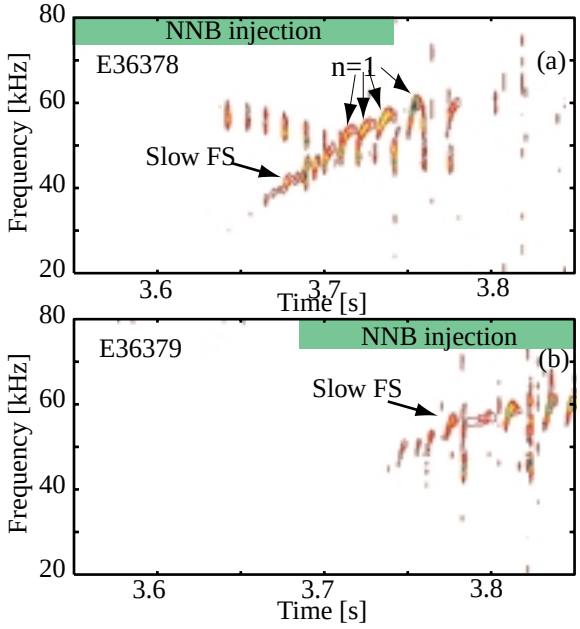

FIG. 3. Time traces of spectrum of magnetic probe. Only start time of N-NB injection is different. N-NB is injected from 3.55 s in (a), and from 3.68 s in (b).

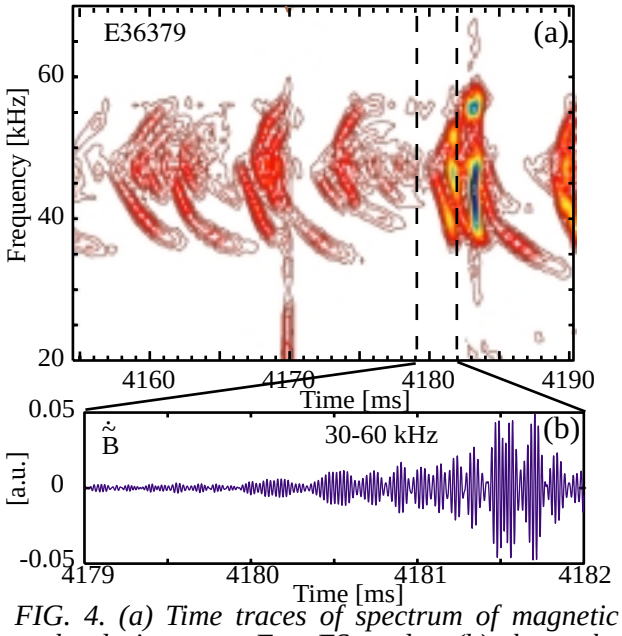

FIG. 4. (a) Time traces of spectrum of magnetic probe during some Fast FS modes. (b) shows the time trace of filtered magnetic probe signal by using numerical band pass filter with a band frequency of 30-60 kHz.

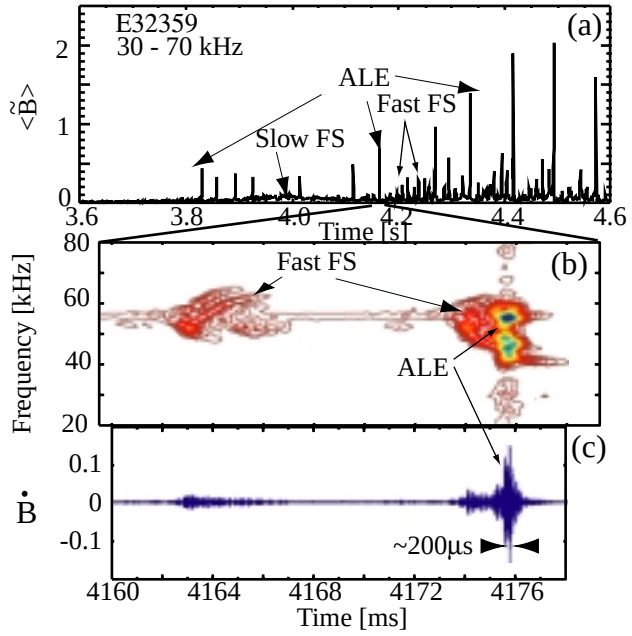

FIG. 5. (a) Time traces of mode amplitude in the frequency range of 30 - 70 kHz. (b) and (c) show the details of one ALE; (b) shows the time trace of frequency spectrum of magnetic fluctuation, and (c) the time trace of filtered signal of magnetic fluctuations within the frequency range of 30 - 70 kHz.

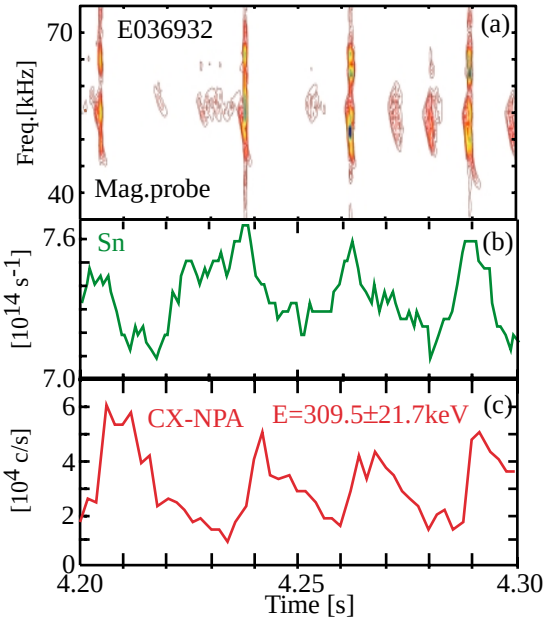

FIG. 6. Time traces of frequency spectrum of magnetic fluctuations, (a), neutron emission rate, (b), and the neutral particle fluxes with the energy of 309.5±21.7 keV measured by CX-NPA, (c).

kHz. These magnetic fluctuation amplitude spikes are called ALEs in this paper because the amplitude signal become large abruptly. The amplitude of most ALEs is typically 2 – 5 times as large as that of Slow FS modes and sometimes becomes $\sim$ 10 times that of Slow FS modes. ALEs appear during the occurrence of Fast FS modes in the most case. Figure 5(b), (c) show the details of one ALE. The ALE has peak amplitude at frequency similar to that of Fast FS modes. ALE grows at the time scale of a few cycles of the mode, $\sim$ 40 – 100 μs and exists in the duration of 200 – 400 μs. It is not clear whether ALE is an instability with a frequency sweep, however we sometimes observe an ALE with a frequency sweeping. As shown in Sec. 3, ALEs cause a large drop of neutron emission rate and an increase in energetic neutral particle fluxes. One candidate for explaining ALE is a nonlinear explosive growing behavior of TAE [6].

3 Loss of energetic ions

Figure 6 shows time traces of (a) frequency spectrum of magnetic fluctuations, (b) neutron emission rate, Sn, and (c) the neutral particle fluxes with the energy of 309.5 $\pm$ 21.7 keV for the discharge E36932. The neutral particle fluxes are measured by a charge exchange neutral particle analyzer (CX-NPA). The CX-NPA installed in JT-60U detects the neutral particles produced from ions whose pitch-angle are almost the same as the injection angle of the N-NB. Figure 6 shows ALE induces drops of neutron emission rate and increases in neutral particle fluxes. In this case, the neutron emission rate drops by about 7 %. The averaged confinement time of energetic ion is estimated by $\langle \tau_c \rangle = T_{\rm MHD}/\ln[1/(1-\Delta Sn/Sn)]$, where $T_{\rm MHD}$ is the interval between MHD activity (ALEs here), and ΔSn is the reduction in neutron emission rate [8]. $T_{\rm MHD} \sim 30$ ms in the case of FIG. 6. The estimated $\langle \tau_c \rangle$ is $\sim$ 0.3 s which is comparable with the slowing-down time, τ_s, of injected ions by N-NB. This corresponds to a loss of the beam power by about 25 % estimated by using the model of $P_{\rm loss}/P_{\rm inj} = 1/(1+\langle \tau_c \rangle/\tau_n)$, where τ_n is the cross-section-weighted beam slowing-down time.

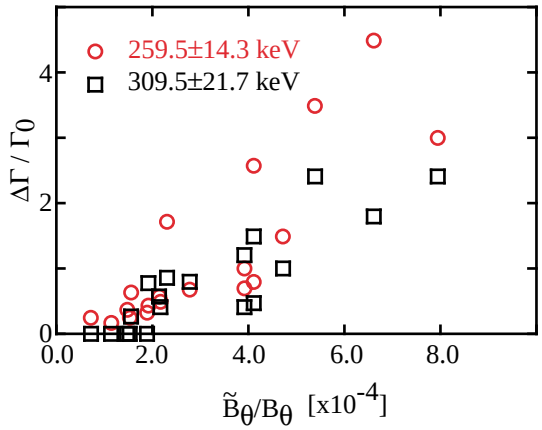

FIG. 7. $\Delta\Gamma/\Gamma_0$ versus the peak magnetic fluctuation amplitude, $\tilde{B_\theta}/B_\theta$, where Γ_0 and $\Delta\Gamma$ are the averaged neutral particle fluxes and the enhancement in neutral particle fluxes, respectively.

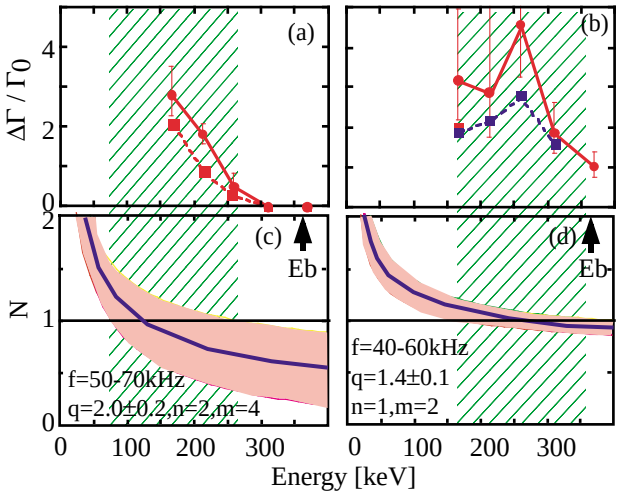

FIG. 8. (a) and (b) show the $\Delta\Gamma/\Gamma_0$ versus the energy of the neutral particle. (c) and (d) show the diagram of the resonant condition,N=(f/f$_C$)q-nq+m, for (a) and (b), respectively. Eb=360keV is the energy of injected N-NB.

Figure 7 shows the increase in neutral particle fluxes, $\Delta\Gamma/\Gamma_0$, versus the peak magnetic fluctuation amplitude, $\tilde{B}_\theta/B_\theta$, where Γ_0 and $\Delta\Gamma$ are the averaged neutral particle fluxes just before ALEs occur and the enhancement in neutral particle fluxes, respectively. The enhanced neutral particle fluxes increase as the amplitude of $\tilde{B}_\theta/B_\theta$ increases. The reduction in neutron emission rate also increases with the amplitude of $\tilde{B}_\theta/B_\theta$ although the scatter of data is relatively large. However we cannot draw a conclusion on the functional dependence because drop of neutron emission rate and increase in neutral particle fluxes are observed in a narrow region of magnetic fluctuations.

Enhanced loss of energetic ions by most of Slow FS modes and Fast FS modes is hardly observed. Sometimes the loss of energetic ions is observed for Fast FS modes when the mode amplitude is large as shown at 4.28 s in FIG. 6. The typical amplitude of these modes, $\tilde{B}_\theta/B_\theta \lesssim$

10^{-4} at the first wall, is not so strong that the mode cannot induce a significant loss of energetic ions.

The energy dependence of the enhanced neutral particle fluxes, $\Delta\Gamma/\Gamma_0$, is observed as shown in FIG. 8(a) and (b). The energy of injected beam, E_b = 360 keV, is also shown by an arrow. In case of (a), the enhanced neutral particle fluxes are observed at the energy of lower than 250 keV. In case of (b), the enhanced fluxes seems to have a peak around 260 keV although the error with lower channels are large. The resonant condition between the mode and the energetic ions is expressed as $N = (f/f_c)q - nq + m$ [9], where N is an integer, f is the mode frequency, f_c is the energetic ion toroidal transit frequency, n is a toroidal mode number, m is a poloidal mode number, and q is the safety factor as shown in FIG. 8(c) for the case of (a) and (d) for the case of (b). The difference between cases (c) and (d) is a observed mode number and the safety factor. The gray area shows the broadness of the resonance condition which is coming from the broadness of mode frequency and the ambiguity of q profile. The range of energy, in which $\Delta\Gamma/\Gamma_0$ increase, qualitatively corresponds to the range of the resonant condition of $N = 1$. Namely, the resonance condition lies around 130 keV in case of (c) and around 260 keV in case of (d). These data suggest that the enhanced neutral particle fluxes result from the resonant interaction between energetic ions and AE modes in ALEs.

4 Summary

Instabilities with frequency sweeping in the frequency range of Alfvén eigenmodes have been found in N-NB injection in JT-60U. Our experiments were performed with energetic ion parameters similar to those of α particles expected for ITER: $0.1\% < \langle\beta_h\rangle < 1\%$ and $v_{b//}/v_A \sim 1$. One type of the observed instabilities, the Slow FS mode, appears with the frequency inside the Alfvén continuum spectrum and its frequency increases to a gap frequency of TAE on the equilibrium change time scale of $\sim$ 200 ms. The frequency of Slow FS modes seems to correlate with the equilibrium parameters of bulk plasma . Another type of the observed instabilities, the Fast FS mode, appears with its frequency in the TAE gap. Most of Fast FS modes consist of several branches with fast frequency chirping; the mode changes its frequency by 10 – 20 kHz in 1 – 5 ms. During the Fast FS mode, abrupt large-amplitude events, ALEs, often appear. Large drop of neutron emission rate and significant increase in fast neutral particle fluxes are observed during these ALEs. The loss of energetic ions increases with the amplitude of $\tilde{B}_\theta/B_\theta$. The loss appears when the peak amplitude of magnetic fluctuation is larger than $\sim 10^{-4}$ at the first wall. Energy dependence of loss ions is observed and suggests the resonant interaction between energetic ions and a mode.

Acknowledgments
The authors would like to thank the members have contributed to the JT-60U project. The authors would like to express our appreciation to Dr. K. Young for his supports to the collaboration between JAERI and PPPL.

References

[1] SIGMAR, D. J. et al., Phys. Fluids B **4** (1992) 1506.

[2] HEIDBRINK, W. W., Plasma Phys. Control. Fusion **37** (1995) 937.

[3] KUSAMA, Y. et al., Nucl. Fusion **39** (1999) 1837.

[4] KRAMER, G. J. et al., Nucl. Fusion **40** (2000) 1383.

[5] GORELENKOV, N. N. et al., Nucl. Fusion **40** (2000) 1311.

[6] BERK, H. L. et al., Phys. Plasmas **6** (1999) 3102.

[7] TODO, Y. et al., Kinetic-magnetohydrodynamic simulation study of fast ions and Toroidal Alfvén Eigenmodes, in *Fusion Energy (Proc. 17th Int. Conf. Yokohama), IAEA-F1-CN-69/THP2/22*, Vienna, 1998, IAEA.

[8] STRACHAN, J. D. et al., Nucl. Fusion **25** (1985) 863.

[9] WHITE, R. B. et al., Phys. Fluids **26** (1983) 2958.